In vivo real-time simultaneous examination of drug kinetics at two separate locations using boron doped diamond microelectrodes

Ai Hanawa, ‡1 Genki Ogata, ‡2 Seishiro Sawamura,2 Kai Asai,1 Sho Kanzaki,3 Hiroshi Hibino,*2 Yasuaki Einaga*1

[1]Department of Chemistry, Keio University, 3-14-1 Hiyoshi, Yokohama 223-8522, Japan

[2]Department of Molecular Physiology, School of Medicine, Niigata University, Niigata 951-8510, Japan

[3]Department of Otolaryngology, School of Medicine, Keio University, 35 Shinanomachi, Shinjuku-ku, Tokyo 160-8582, Japan

‡Contributed equally

*Corresponding authors

E-mail address: einaga@chem.keio.ac.jp

KEYWORDS Methylcobalamin, Real-time detection, Drug kinetics, Boron-doped Diamond, Microelectrodes

ABSTRACT: Methylcobalamin, which is used for the clinical treatment of patients with neuropathy, can have an impact on the sensorineural components associated with the cochlea and it is possible that the auditory threshold in a certain population of patients with deafness may be recovered. Nonetheless, it remains uncertain whether the action site of methylcobalamin is localized inside or outside the cochlea and which cellular or tissue element is targeted by the drug. In the present work, we developed a method to realize *in vivo* real-time simultaneous examination of the drug kinetics in two separate locations using boron-doped diamond (BDD) microelectrodes. First, the analytical performance of methylcobalamin was studied and the measurement protocol was optimized *in vitro*. Then, the optimized protocol was applied to carry out real-time measurements inside the cochlea and leg muscle in live guinea pigs while systemically administering methylcobalamin. The results showed that, methylcobalamin concentration in the cochlea was below the limit of detection for the microelectrodes or the drug did not reach the cochlea, whereas the compound clearly reached the leg muscle.

Introduction

Vitamin B_{12} is an organometallic compound that contains a cobalt-carbon bond and plays a pivotal role in a variety of biological processes such as the production of red blood cells and the synthesis of DNA.[1] Methylcobalamin, an active form of vitamin B_{12}, is necessary for the maintenance of the peripheral nervous system and, as such, is used for the clinical treatment of patients with different types of neuropathy.[2] In several Asian countries, administration of this reagent is a typical pharmacotherapy used to treat sensorineural hearing loss, which is caused primarily by a disorder of the inner ear, in particular, the cochlea.[3] The cochlea comprises three compartments that are filled with different extracellular solutions and is made up of sensory hair cells, neuronal fibers, ganglion neurons, epithelial cells, fibrocytes, and an extracellular matrix. The mechanical energy of sound is converted by the hair cells into electrical signals, which are transmitted through the afferent auditory nerve to the central nervous system.[4] The cochlea is also innervated and functionally controlled by the efferent nerve that originates from the brainstem.[5] Systemically administrated methylcobalamin may affect the sensorineural components associated with the cochlea and it is likely that the auditory threshold in certain populations of patients with deafness can be recovered.[6] Nonetheless, it remains uncertain whether the action site of methylcobalamin is localized inside or outside the cochlea and which cellular or tissue element is targeted by the drug. In addition, with pharmacotherapy, it is important to carry out *in vivo* studies of the changes in drug concentration in a number of separate locations, especially in real time; however, no such analysis has yet been attempted using conventional approaches.

Methylcobalamin can be measured by high performance liquid chromatography/inductively coupled plasma mass spectrometry[7,8] as well as chemiluminescence analysis.[7,9] These methods require manual harvesting of the analytes and so have low sampling rates. Moreover, the collection of multiple samples from a tiny cochlea (size: 1.5–5 mm in rodents) might, over time, damage its fine structure, interfering with the stable and continuous monitoring of the drug concentration in live animals. Electrochemical techniques can track the behavior of chemical compounds over time with high time resolution.[10,11] In this context, methylcobalamin is detectable *in vitro* with mercury, gold, or silver electrodes.[12-15] Nevertheless, the size of each of these classical electrodes is too large for *in vivo* analysis in a cochlear

microenvironment. Biocompatible carbon fiber electrodes may be applicable for local measurements; however, this is unlikely to be suitable for longitudinal detection of the drug, due to its fragility, unstable response and relatively high background noise.[16]

On the other hand, boron-doped diamond (BDD) electrodes are attracting increasing attention as one of the next-generation of electrode materials.[17-21] The superior electrochemical properties of BDD electrodes, such as the wide potential window in aqueous solutions and the low background current make it particularly attractive for use in highly sensitive electroanalysis.[22] In addition, the high chemical and physical durability of the sp^3 hybridized structure, good biocompatibility, the rapid and stable response, and the high resistance to non-specific absorption make BDD an excellent choice as an electrode. Furthermore, needle-like BDD microelectrodes with small electroactive areas can be fabricated, and they have unique properties such as spherical diffusion, an increased rate of mass transport, and reduced capacitance allowing a fast response.[16,23-29] Moreover, the sample volume required for these microelectrodes need only be very small, so it is possible to carry out sensitive analytical *in vivo* studies in local areas by using microelectrodes with tip diameters of 5-20 μm. In our earlier work, BDD microelectrodes were inserted into the cochlea of a guinea pig and into the brain of a rat, and we succeeded in making real-time measurements of changes in concentration of a few different drugs, which were intravascularly injected into the animals. [30]

On the basis of this technique, in the present work, we developed a novel system with two BDD microelectrodes that allows us to simultaneously examine two separate local areas *in vivo*. In order to realize the system, first, we investigated the electrochemical reaction of methylcobalamin including the analytical performance using BDD microelectrodes and optimized the measurement protocol *in vitro*. Then, the optimized protocol was applied to carry out real-time measurements inside the cochlea and a leg muscle in live guinea pigs that were systemically administrated with methylcobalamin. An anticancer drug, doxorubicin, when vascularly applied, is detected in the guinea-pig cochlea by BDD microelectrodes[30]; therefore, this drug was sequentially administrated after the injection of methylcobalamin to verify the electrodes in the cochlea and muscle. A clear difference between the uptake of the drug in the two regions was revealed.

Experimental Section

Preparation of boron-doped diamond (BDD) electrodes

The method used to prepare the BDD electrodes was similar to that given in our previous reports.[22, 23, 30] Briefly, polycrystalline BDD films were deposited on silicon wafers and on tungsten wires to fabricate plate electrodes and microelectrodes, respectively. For microelectrodes, initially, the 50 or 100 μm diameter tungsten wires were electropolished in a solution of 2 M KOH to achieve a conical shape. The deposition was done in a microwave plasma-assisted chemical vapor deposition (MPCVD) system (AX5250M, Cornes Technologies, Ltd.), with plasma powers of 5.0 kW and 3.0 kW applied for 6 h and 2h with deposition pressures of 100 Torr and 60 Torr, respectively. A mixture of acetone and trimethoxyborane was used for the carbon and boron sources with a boron/carbon ratio of 1%. The surface morphology and crystalline structure was characterized using scanning electron microscopy (SEM) (JCM-6000 plus, JEOL, Ltd.) (Figure S11(a)(b)). The film quality was confirmed by Raman spectroscopy (Acton SP2500, Princeton Instruments, Inc.) (Figure S11(c)(d)). The BDD microelectrodes were insulated with glass capillaries to define the electrode surface area. A capillary (G-100, Narishige) was pulled by capillary puller (PC-10, Narishige). The tip of the capillary was then cut by microforge (MF-900, Narishige) to cover the BDD needle with the tip extruding by ca. 100–200 μm. The capillary-covered BDD needle was heated at ca. 700 ºC for 30 s in argon atmosphere. The capillary was evacuated by a diaphragm pump (DIVAC 0.6L, Lenbold) during the heating. This procedure was necessary for a tight seal between the BDD and the glass capillary (Figure SX). Then, copper wires were connected to the microelectrodes with silver paste. The details of the preparation have been described previously. The sizes of the conducting tips of the electrodes were < 30 μm in diameter and 50-300 μm in length.

Chemicals

Methylcobalamin and potassium hexacyanoferrate(II) trihydrate ($K_4[Fe(CN)_6]$) were purchased from FUJIFILM Wako Pure Chemical Corporation and used without any purification. A 0.1 M phosphate buffer (PB) solution with pH 7.4 was used as the electrolyte. This solution contained 19 mM sodium dihydrogen phosphate (NaH_2PO_4) and 81 mM sodium hydrogen phosphate (Na_2HPO_4). A 1 M aqueous solution of sulfuric acid (H_2SO_4) was used to clean the BDD electrode by cathodic reduction. All the solutions were prepared with pure water supplied from DIRECT-Q 3 UV (Merck Millipore Corp.) with a specific resistivity of 18.2 MΩ·cm.

In vitro electrochemical measurements

Electrochemical measurements were carried out using a potentiostat (ALS 852cs, BAS Inc.) controlled by a laptop computer. Initially, cyclic voltammetry (CV) was conducted with the potentiostat using a single-compartment three-electrode polytetrafluoroethylene (PTFE) cell with an Ag/AgCl (saturated KCl) reference electrode and a coiled Pt wire counter electrode. The electrical contacts for the electrochemical measurements were made by connecting copper wires to the BDD surface with silver paste. The BDD (Pt and GC) electrode was fixed with an O-ring (electrode area: 0.36 cm2) and connected to the potentiostat through a copper plate placed under the working electrode.

For continuous measurements, a BDD microelectrode was used as the working electrode. The 3 electrodes (working electrode, counter electrode and reference electrode) were immersed in a beaker containing 5 ml of phosphate buffer solution (Figure S4). Three different measurement protocols were examined. For each protocol, stock solutions of methylcobalamin were added to the PB solution in the beaker, which was then stirred with a magnetic bar for 3 seconds.

In vivo measurements of methylcobalamin

Each BDD microelectrode was used for only one series of *in vivo* measurements in a guinea pig and was not used in other animals. Before being used in an *in vivo* experiment, the microelectrode was immersed in a 1 M H_2SO_4 solution and 3.0 V (vs. Ag/AgCl) was applied for 30 s and subsequently −4.0 V (vs. Ag/AgCl) for 1200 s. With these anodic and cathodic pretreatments, the BDD surface was rid of any impurities and dominated by hydrogen termination. The electrode was then subjected to a cyclic voltammetry protocol (sweep rate, 0.1 V/s; potential window, −1.0 V to 1.5 V (vs. Ag/AgCl); and initial potential, 0.0 V (vs. Ag/AgCl)) in PB solution until the background signal became stable. Thereafter, a calibration curve for the microelectrode was determined *in vitro*. Any electrode which failed to have a slope ≥ 1.0 was discarded.

Healthy male Hartley guinea pigs (350–700 g, 2–12 weeks old; SLC Inc., Hamamatsu, Japan), the hearing levels of which were evaluated in advance by Preyer's reflex test and confirmed to be normal, were used for the *in vivo* experiments. Urethane (1.5 g kg^{-1}, Sigma-Aldrich Japan, Tokyo, Japan) was intraperitoneally injected into the animals for deep anesthesia. The depth of the anesthesia was continuously monitored with a toe pinch, the corneal reflex, and the respiratory rate. During the recording, the body temperature was maintained at 37 °C on a heating blanket (BWT-100A, BioResearch Center, Nagoya, Japan). To inject methylcobalamin, an ethylene tetrafluoroethylene tube was inserted into the right external jugular vein of each guinea pig. 5 mg of methylcobalamin was dissolved in 1 ml of PB solution immediately before being injected into each guinea pig for the *in vivo* measurements; the dosage was 10 mg kg^{-1} for each guinea pig.

Results and Discussion

Electrochemical reduction of methylcobalamin

Cyclic voltammograms (CVs) of 100 μM methylcobalamin with a normal amount of dissolved oxygen using a BDD disk electrode are shown in Figure 1. The experimental methods can be found in Supporting Information. The reduction potential of methylcobalamin is at −0.7 V (vs. Ag/AgCl) and the reduction potential of the dissolved oxygen is at −0.9 ~ −1.0 V (vs. Ag/AgCl). In order to understand the mechanism of the reduction reaction, CVs of 100 μM methylcobalamin in degassed by nitrogen and oxygen saturated 0.1 M phosphate buffer solutions were also measured (Figure S2(b) and Figure S2(d), respectively). When oxygen is present, two reduction peaks (−0.7V~−0.8V and −0.8~−0.9V (vs. Ag/AgCl)) are observed, while no peaks are observed without oxygen (Figure S2(b)). The normal situation with dissolved oxygen (6-8 mg/L at 20 °C) also has two similar reduction peaks (Figure 1(b), Figure S2(c)). The reduction peaks can be explained by a catalytic mechanism involving oxygen reduction.[31-33] It is suggested that, in the initial part of the negative scan, Co(II)-O_2, in which O_2 is an axial ligand of Co(II), is reduced to Co(II)-H_2O_2 (which can be Co(II) and H_2O_2) by two-electron reduction (Scheme S1 (1)). The observed first peak at −0.7V~−0.8V (vs. Ag/AgCl) can be assigned as the two-electron reduction. Then, as the potential goes more negative, H_2O_2 can be reduced to H_2O. Furthermore, when the potential reaches around −0.8 V (vs. Ag/AgCl), the inert Co(II) is reduced to Co(I) with the molecular oxygen fixed axially to Co (Co(I)-O_2). At more negative potentials, direct four-electron reduction of Co(I) and H_2O can occur. The observed second peak (−0.8~−1.2 V (vs. Ag/AgCl)) can be assigned as the overlapping of these reactions (Scheme S1 (2)-(4)). Although the reduction mechanisms are complicated, it is possible to determine the concentration of methylcobalamin from the first reduction peak at −0.7V~−0.8V (vs. Ag/AgCl).

To compare the performance of BDD electrodes with conventional electrode materials, CVs were obtained using glassy carbon (GC) and Pt electrodes, respectively (Figure S3). Since the background current was much higher with GC than with the BDD electrode, the reduction response is not as clear as that observed using the BDD electrodes. In the case of the Pt electrode, the reduction peak cannot be observed because the surface of the Pt can be easily poisoned to form PtO. (Figure S2(a3)).[34] Accordingly, the signal to background ratios were 4.7, 1.4, and 1.1, for the BDD, GC, and Pt electrodes, respectively (Figure S3(b)).

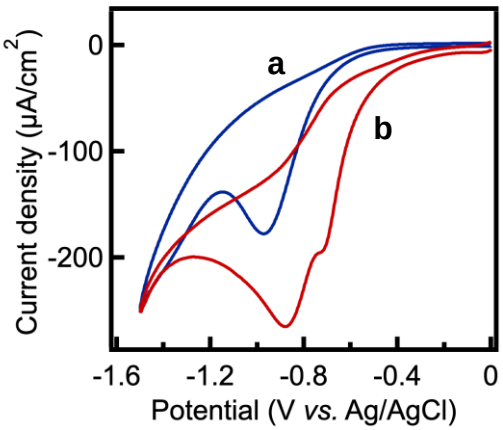

Figure 1. Cyclic voltammograms (CVs) of 0.1 M phosphate buffer (PB) solution at a scan rate of 0.1 V/s (a) in the absence and (b) in the presence of 100 μM methylcobalamin using a BDD disk electrode.

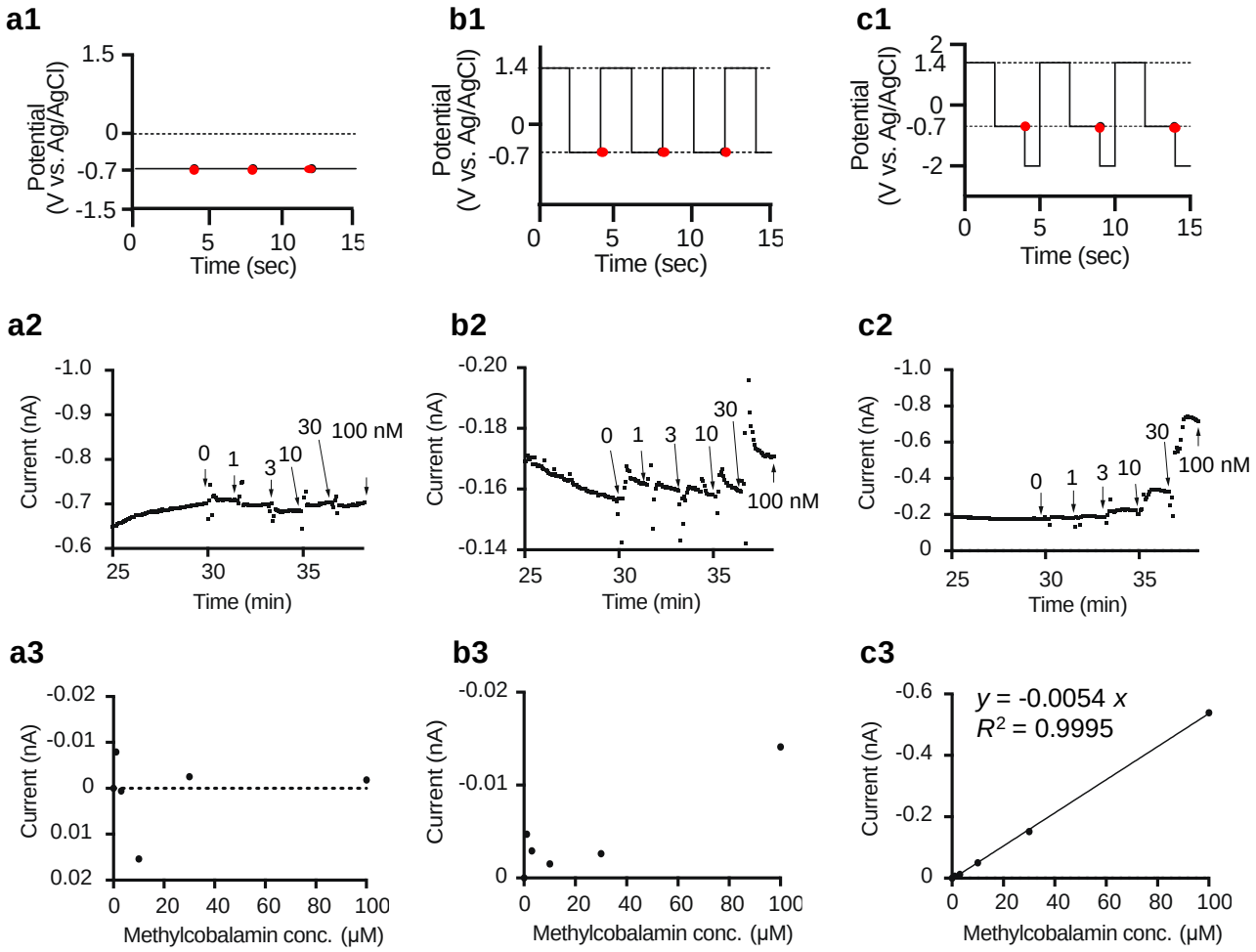

Figure 2. Optimization of the in vitro measurement protocol.

(a) Protocol A: (a1) The chronoamperometry protocol. The electrode potential was fixed at −0.7 V (vs. Ag/AgCl), and the current was monitored every 4 seconds (red points); (a2) Amperometric response. Methylcobalamin (0, 1, 3, 10, 30, 100 nM dissolved in PB solution) was added in stages. The measurements were made when the current had reached a steady state, and is shown by the arrows; (a3) The variation in steady-state current with methylcobalamin concentration.

(b) Protocol B: (b1) The two-step protocol. Potentials of +1.4 V (vs. Ag/AgCl) for 2 seconds and −0.7 V (vs. Ag/AgCl) for 2 seconds were applied to the electrode, and the current was monitored every 4 seconds (red points); (b2) Amperometric response. Methylcobalamin (0, 1, 3, 10, 30, 100 nM dissolved in PB solution) was added in stages. The measurements were made when the current had reached a steady state, and is shown by the red arrows; (b3) The variation in steady-state current with methylcobalamin concentration.

(c) Protocol C: (c1) The three-step protocol. Potentials of +1.4 V (vs. Ag/AgCl) for 2 seconds, −0.7 V (vs. Ag/AgCl) for 2 seconds, and −2.0 V (vs. Ag/AgCl) for 1 second were applied to the electrode. The current was monitored every 5 seconds (red points)., (c2) Amperometric response. Methylcobalamin (0, 1, 3, 10, 30, 100 nM dissolved in PB solution) was added in stages. The measurements were made when the current had reached a steady state, and is shown by the red arrows; (c3) The variation in steady-state current with methylcobalamin concentration. The slope and r^2 of the regression line are shown.

Optimization of the in vitro measurement protocol

In order to optimize the measurement protocol for *in vivo* measurements, continuous *in vitro* measurements by chronoamperometry were conducted using BDD microelectrodes (Figure S4). Here, 3 different protocols (1 step, 2 steps, and 3 steps) were investigated (Figure 2(a1), 2(b1), and 2(c1)). For each protocol, the current at the reduction potential of methylcobalamin, −0.7 V (vs. Ag/AgCl) (red points) was measured, after the adding drops of methylcobalamin. Calibration curves, i.e., the dependence of current on the concentration of methylcobalamin, is plotted for each protocol in Fig. 2(a3), 2(b3), and 2(c3).

Protocol A is a single-step process. The potential was fixed at −0.7 V (vs. Ag/AgCl), and the current was monitored every 4 seconds. The background current increased gradually even without methylcobalamin (Figure 2(a2)), and the

current with methylcobalamin was unstable and independent of the concentration (Figure 2(a3)). Protocol B is a two-step process. In order to supply oxygen and to stabilize the background current, a positive potential (+ 1.4 V (vs. Ag/AgCl)) was applied for 2 seconds before the measurements at −0.7 V (vs. Ag/AgCl). Protocol C is a three-step process. After the measurements at −0.7 V (vs. Ag/AgCl), −2.0 V (vs. Ag/AgCl) was applied for 1 second to initialize the surface termination to hydrogen.

The relative standard deviation of the background current for 200 seconds before adding drops of the methylcobalamin indicates that the current measured using Protocol C was more stable compared to Protocols A and B (Figure 2, Figure S5). Furthermore, a good linear calibration curve was obtained for Protocol C. To initialize the surfaces of the BDD electrodes, control of the surface termination is important, because the electrochemical performance depends on the surface termination.[35-37]

Typical surface terminations are hydrogen-termination and oxygen-termination. BDD produced by chemical vapor deposition (CVD) system is terminated by hydrogen due to synthesis in a hydrogen ambient. The hydrogen termination can be oxidized to oxygen-termination by anodic oxidation (AO) treatment or exposing the BDD to an oxygen plasma, and so on. On the other hand, the conversion from oxygen-termination to hydrogen-termination can be achieved by cathodic reduction (CR) or exposing it to a hydrogen plasma.

When the measurement is made, the surface should always have identical termination to give accurate current values. When the surface termination is unstable, incorrect values are obtained. First, we need to understand how the surface termination varies using Protocols A, B, and C. Here, CVs of a 1 mM $K_4[Fe(CN)_6]$ redox couple were measured. After operation for 1 hour, the CVs were acquired again just before collecting the data (at −0.7 V (vs. Ag/AgCl)) (Figure 3). The separations between the peaks, ΔE_p, are summarized in Figure 3(b). With Protocol A and C, the values of ΔE_p were identical before and after operating for 1 hour (Figure 3(a1), 3(a3)). In contrast, for Protocol B, ΔE_p increased from 86 mV to 168 mV after 1 hour operation, suggesting that the BDD surface had become more oxygen-terminated (Figure 3(a2)). That is, we demonstrated that the application of alternate positive and negative potentials in addition to applying the methylcobalamin reduction potential (−0.7 V vs. Ag/AgCl) successfully maintained the BDD surface termination. Because, moreover, the calibration curve (methylcobalamin concentration dependence) for Protocol C shows good linearity (Figure 2(c3)), Protocol C (three-step process) was selected as the optimum one.

Next, each parameter in Protocol C, i.e. the positive potential, the measurement potential, and the negative potential, was optimized.

First, the applied positive potential was optimized by CV measurements after applying various positive potentials from 0.0 V to +1.5 V. The current obtained at −0.7 V (vs. Ag/AgCl) after the various applied potentials is plotted in Figure S5. Higher currents were obtained when the applied potential was more than +0.8 V (vs. Ag/AgCl). Thus, the optimum applied potential was fixed at +1.4 V (vs. Ag/AgCl). Note that oxygen generated by the positive potential can also contribute to the reduction reaction of methylcobalamin at −0.7V∼−0.8V (vs. Ag/AgCl) via a catalytic mechanism involving oxygen reduction, as mentioned above. The results in Figure S6 suggest that the oxygen contribution can be generated by applying potentials greater than +0.8 V (vs. Ag/AgCl), so the oxygen generation at +1.4 V (vs. Ag/AgCl) is beneficial. That is, application of a positive potential not only provides the means for oxidation of the surface (change in termination) but also enables the generation of catalytic oxygen for the methylcobalamin reduction reaction.

Second, the measurement potential for data collection, i.e., the reduction potential of methylcobalamin, was optimized by making measurements in the range from −0.6 V (vs. Ag/AgCl) to −1.0 V (vs. Ag/AgCl) (Figure S7). With potentials from −0.8V to −1.0 V (vs. Ag/AgCl), the calibration curves were nonlinear due to interference by the oxygen reduction reaction (Figure S7(a3), S7(a4)). Linear calibration curves were obtained in the case of −0.6 V and −0.7 V (vs. Ag/AgCl) (Figure S7(a1), S7(a2)), and the best analytical performance was obtained at −0.7 V (vs. Ag/AgCl) (Figure S7(a2)), which showed less errors and a low limit of detection (LOD) of 0.09 nM (Figure S7(b) and S7(c)). Therefore, the optimum measurement potential for data collection was fixed at −0.7 V (vs. Ag/AgCl).

Third, the applied negative potential was optimized in the range from −1.0 V (vs. Ag/AgCl) to −2.0 V (vs. Ag/AgCl) (Figure S8). The best result was obtained with the potential at −2.0 V (vs. Ag/AgCl), while the calibration curves at −1.0 V (vs. Ag/AgCl) and −1.5 V (vs. Ag/AgCl) were nonlinear. Electrochemical cathodic reduction with BDD electrodes at negative potentials has been widely used to hydrogenate surfaces to obtain hydrogen termination.[30] The results are consistent with those given in our previous report in which we showed that a negative potential was needed for hydrogenation by cathodic reduction.

Taking the above results into account, the optimum protocol has the potential held at +1.4 V (vs. Ag/AgCl) for 2 s, stepped to −0.7 V (vs. Ag/AgCl) for 2 s, and then stepped to −2.0 V (vs. Ag/AgCl) for 1 s.

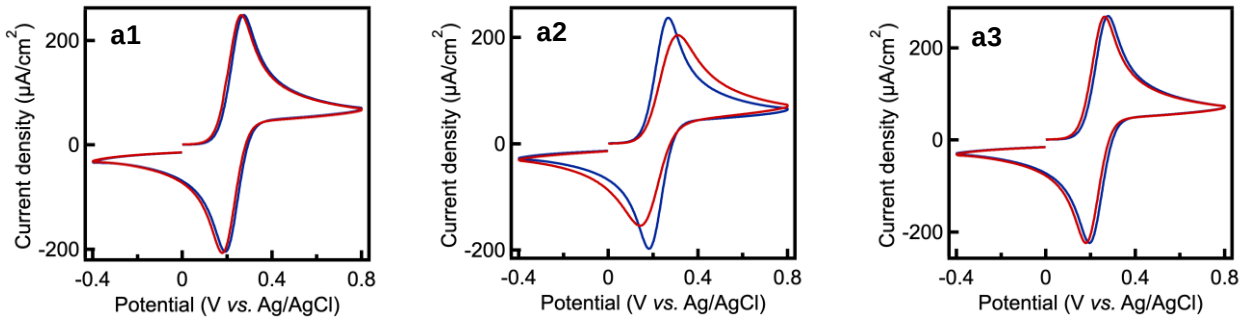

b

Protocol	*ΔE*p (mV)	
	Before operation	After operation
A (1step)	82	84
B (2steps)	86	168
C (3steps)	84	84

Figure 3. Cyclic voltammograms in aqueous solutions of 1 mM $K_4[Fe(CN)_6]$ in 0.1 M phosphate buffer (PB) solution before and after operation for 1 hour using (a1) Protocol A, (a2) Protocol B, and (a3) Protocol C, respectively. The scan rates were 0.1 V/s. (b) The peak separation (ΔE_p) before and after operation.

In vivo measurement of methylcobalamin in the cochlea

Before the *in vivo* experiment, the calibration curve for methylcobalamin (1–10 nM) was acquired for each BDD microelectrode in vitro (Figure 4(a)(b)). The optimum protocol (Protocol C) was used. Linear calibration curves for the methylcobalamin concentration were obtained for each BDD microelectrode, although the sensitivities of these were not the same due to individual differences between them (Figure 4(b)).

We then used the BDD microelectrodes to determine whether or not systemically administrated methylcobalamin can reach the cochlea in the inner ear of a guinea pig. The cochlea has a snail-like structure with three tubular chambers, which spiral from the base to the apex (Figure 4(c)). Two chambers, the scala tympani and scala vestibuli, contain perilymph whose ionic composition is similar to regular extracellular fluid, whereas the other chamber, the scala media, is filled with a K^+-rich extracellular fluid, endolymph. There are several elements crucial for the correct neuronal function in the cochlea, including the sensory hair cells, ganglion neurons and the nerve fibers connecting these two components together. These are bathed in the perilymph of the scala tympani,[38,39] so this space was selected as the target for the measurement. For comparison, we simultaneously monitored the response to the drug in the gracilis muscle of the right hind leg. For this, we used an integrated system comprising two BDD microelectrodes (Figure 4c; also see Experimental Methods in Supporting Information).

One of the BDD microelectrodes was inserted into the cochlear perilymph of an anesthetized guinea pig while the other was inserted into the extracellular space of a leg muscle in the same guinea pig (Figure 4c). Under controlled conditions, cyclic voltammograms with the microelectrodes at each of these locations showed prominent anodic currents at potentials exceeding approximately 0.4 V (vs. Ag/AgCl) (Figure S9). Negligible cathodic current was observed at negative potentials. These characteristics were deemed unlikely to interfere with electrochemical measurements of methylcobalamin, because the current arising in the presence of this drug occurs at negative potentials (at −0.7 V (vs. Ag/AgCl) in the *in vitro* study (see Figure 1)).

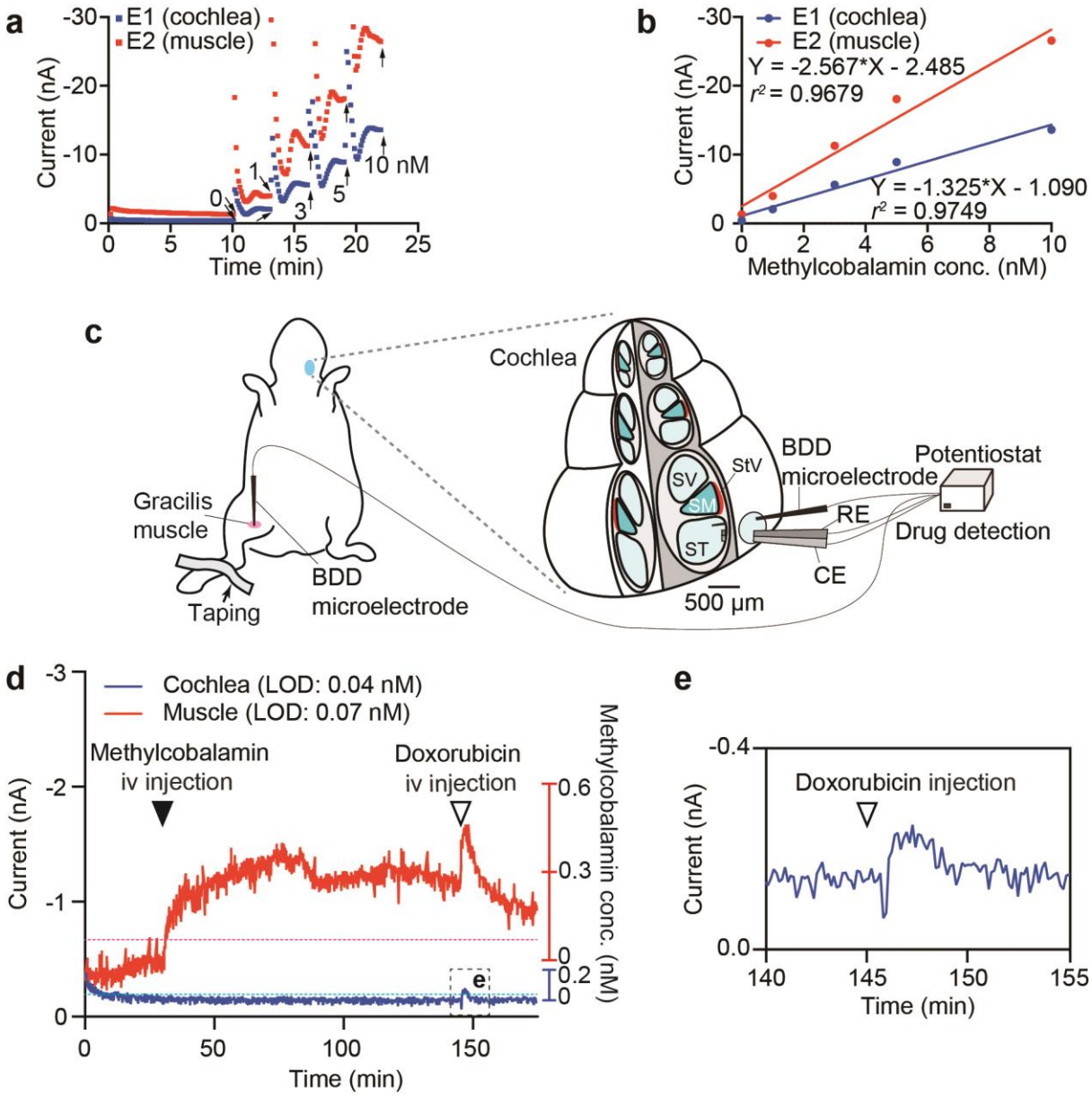

Figure 4. *In vivo* detection of methylcobalamin in a guinea pig.

(a and b) *In vitro* calibration of the BDD microelectrodes for measurements in the cochlea (electrode E1) and leg muscle (electrode E2). The protocol provided for the electrodes was Protocol C (Figure 2(c1)) (+1.4 V (vs. Ag/AgCl) for 2 seconds, −0.7 V (vs. Ag/AgCl) for 2 seconds, and −2.0 V (vs. Ag/AgCl) for 1 second)). Methylcobalamin (1−10 nM dissolved in PB solution) was added incrementally to the electrolyte; the cathodic current at −0.7 V (vs. Ag/AgCl) for each drug concentration was measured (red points in Figure 2(c1)). The steady-state current (shown by the arrows in (a)) is plotted against the drug concentration in (b). The slope and r^2 of the regression line for each electrode are shown.

(c) The in vivo experimental setup. A schematic illustration of the cochlea is shown on the right. The system we developed included two boron-doped diamond (BDD) microelectrodes; each electrode was inserted into the perilymph in the scala tympani (ST) or into the extracellular space in the gracilis muscle of the right hind leg. A microcapillary containing the reference and counter electrodes (RE and CE) was placed in the ST in the vicinity of the BDD microsensor. SM; scala media, SV; scala vestibuli, StV; stria vascularis.

(d and e) *In vivo* assay in a live guinea pig. The current in the cochlear perilymph of the scala tympani (blue) and that in the leg muscle were measured with the calibrated BDD microelectrodes E1 and E2, respectively. Protocol C (Figure 2(c1)) was applied to the microelectrodes. 10 mg kg^{-1} methylcobalamin was injected into the right external jugular vein 30 min (filled arrowhead in (d)) after starting recording. Then, 5 mg kg^{-1} doxorubicin was injected via the same route. The trace in the boxed region in (d) is enlarged in panel (e). Methylcobalamin concentrations in the cochlea and the muscle (blue and red

axes, respectively, on the right hand side) were obtained using the calibration curves in (b), as mentioned in the main text. The blue and red dotted lines indicate the '*in vivo*' limits of detection for microsensors E1 and E2, respectively. These values were obtained as described in 'Experimental Methods'(Supporting Information).

For local measurement of the methylcobalamin (Figure 4d), we switched to the aforementioned chronoamperometry conditions and the steady-state response at −0.7 V (vs. Ag/AgCl) was recorded every 5 seconds. The background current measured in the absence of the drug gradually changed and became stable around 15 min after the start of recording. A solution containing methylcobalamin (10 mg kg^{-1}) was injected into the left external jugular vein in the guinea pig 30 min after starting recording. In the cochlear perilymph, little action was observed over a period of 120 min after injection. On the other hand, there was a marked response in the muscle, as follows. The current began to increase immediately after injection of the drug and reached a maximum of −1.3 nA in approximately 45 min. Then, there was a gradual and moderate decrease in current. To estimate the drug concentration from the *in vivo* response, the average value of the background current recorded for 10 min before injection was set as the baseline for the calculation by means of the calibration curves shown in Figure 4b. The maximum drug concentration during the measurement in the muscle was 0.4 μM (Figure 4d, right y axis). Furthermore, 150 min after starting recording, doxorubicin (5 mg kg^{-1}), which has been found in *in vitro* experiments to give rise to a cathodic current with a BDD electrode at −0.7 V (vs. Ag/AgCl),[30] was injected into the vein (Figure 4d). The injection resulted in a rapid and immediate increase in current in both the cochlea and the muscle. This observation in the cochlea was similar to the result obtained in our earlier work (Figure 4e).[30]

The magnitudes and patterns of the background noise in the cochlear perilymph and the leg muscle are clearly different. Furthermore, the properties of the BDD microelectrode used in the cochlea differed from those of the BDD microelectrode used in the muscle. Therefore, for the experiment illustrated in Figure 4d, we calculated the '*in vivo*' limit of detection (LOD) for each microelectrode from the background current and the slope of the *in vitro* calibration curve (see Methods in Supporting Information). In the cochlea, the measurements from the time of methylcobalamin injection to that of doxorubicin injection never reach the LOD value. On the other hand, in the muscle most of the measurements clearly exceed the LOD value. The pharmacokinetics, i.e., declining kinetics of methylcobalamin in the leg muscle in Figure 4d is discussed in Supporting Information (see also Figure S12 and Table S1 in Supporting Information).

In the *in vivo* experiment described above, the sensitivity to the drug of the BDD microelectrode in the cochlear perilymph was lower than that for the muscle (Figure 4(a)(b)). In light of this, two additional guinea pigs were tested for local measurements of methylcobalamin with the same experimental protocol as in Figure 4. In each guinea pig, we used a pair of different BDD microelectrodes characterized as follows; the slope of the calibration curve of the microelectrode used for the cochlea was larger than that used for the muscle (Figure S10(b)(e)). As shown in Figure S10(c)(f), the results obtained at the two separate locations in both animals were similar to the observation displayed in Figure 4d. Parameters characterizing in vivo pharmacokinetics of methylcobalamin in the muscle for three tested animals are described in Supporting Information (Figure S11 and Table S1). Considering all these results, we can conclude that the concentration of the drug was below the detection limit of the BDD microelectrodes in the perilymph but it was clearly measured in the muscle.

The clinical dose for single administration of methylcobalamin is typically 500 μg or approximately 10 μg kg^{-1}.[40] In this study, when a larger dose (10 mg kg^{-1}) was intravenously injected into normal guinea pigs, the concentration in the cochlear perilymph of the scala tympani never exceeded the LOD of the BDD microelectrodes (0.006–0.04 nM) (Figure 4 and Figure S10). Therefore, the amount of the drug reaching the cells and tissues immersed in the perilymph, such as the sensory hair cells, neuronal fibers, and ganglion neurons, was likely to be negligible. Thus, the function of the blood-labyrinth barrier can be compared to that of the blood-brain barrier, which allows the permeation of compounds with molecular weights up to 400–800 g mol^{-1} [41,42]; this maximum limit is less than the molecular weight of methylcobalamin (1344.4 g mol^{-1}).[43] On the basis of these observations, the likely target(s) of methylcobalamin are the following. The first candidates are the afferent and/or efferent nerves outside the cochlea. Secondly, the drug could pass through the capillary endothelial cells of the epithelial tissue, the stria vasularis, and be conveyed into the endolymph in the scala media (see Figure 4c), where the apical surfaces of sensory hair cells are exposed. Indeed, on this pathway systemically administrated aminoglycosides enter the hair cells and destroy them.[44] Alternatively, we cannot rule out the possibility that a metabolite of methylcobalamin that is undetectable by the BDD microelectrode, can reach inside the cochlea and elicit a therapeutic activity. In addition, the pathological sources for deafness such as inflammation, virus or bacterial infection, and acoustic trauma, may modulate the structure of the blood-labyrinth barrier and increase the permeability for methylcobalamin. Further studies using the microsensing system developed in this study will enable us to more precisely determine the target of the drug and help clarify the mechanism of the pharmacotherapeutic process.

Conclusions

In the present work, we developed a novel method to realize *in vivo* real-time simultaneous examinations of the drug kinetics at two separate locations using boron-doped diamond (BDD) microelectrodes. An optimized protocol was applied to carry out real-time measurements inside the cochlea and leg muscle in live guinea pigs that were systemically administrated with methylcobalamin. It was found that the amount of methylcobalamin reaching the cochlea was likely to be negligible, while it does reach the leg muscle. The results of this study demonstrate that it is possible to make "in vivo real-time simultaneous examinations of drug kinetics at a number of separate locations in various organs".

ASSOCIATED CONTENT

Supporting Information. The supporting information is available free of charge via the Internet at http://pubs.acs.org. Experimental methods, electrochemical measurements including cyclic voltammograms and optimization of the applied potential, *in vivo* electrochemical detection in different guinea pigs, SEM images and Raman spectra.

AUTHOR INFORMATION

Corresponding Authors

*Y.E. einaga@chem.keio.ac.jp; *H.H. hibinoh@med.niigata-u.ac.jp

ORCID
Genki Ogara: 0000-0003-1753-428X
Seishiro Sawamura: 0000-0002-3713-303X
Kai Asai: 0000-0002-2885-7116
Sho Kanzaki: 0000-0001-9056-0850
Hiroshi Hibino: 0000-0003-0688-1489
Yasuaki Einaga: 0000-0001-7057-4358

Author Contributions

‡A.H and ‡G.O. contributed equally. A.H., G.O., S.S, H.H. and Y.E. designed the experiments. A.H. and G.O. developed the experimental setup. A.H., K. A. and Y.E. prepared the BDD electrodes. A.H. and K.A. performed the electrochemical experiments in vitro, while A.H., G.O. and S.S. performed the in vivo experiments. A.H., G.O., S.S., K.A., S.K., H.H. and Y.E. analyzed the results. A.H., G.O., H.H. and Y.E. wrote the manuscript. All authors edited the manuscript and have given approval to the final version of the manuscript.

Notes

The authors declare no competing financial interest.

ACKNOWLEDGMENT

This study was partially supported by the following research grants: JST-ACCEL (to Y.E.), Grant-in-Aid for Scientific Research A 19H00832 (to Y.E.), Grant-in-Aid for Scientific Research A 18H04062 (to H.H.), Grant-in-Aid for Scientific Research B 18H03513 (to G.O.) and Grants-in-Aid for Young Scientists B 17K17736 (S.S) from the Ministry of Education, Culture, Sports, Science, and Technology of Japan. In addition, funds were kindly provided by The Nakatani Foundation (to H.H. and Y.E.), Takeda Science Foundation (to G.O.), The Mochida Memorial Foundation for Medical and Pharmaceutical Research (to G.O.), Fukuda Foundation for Medical Technology (to G.O.), Nishinomiya Basic Research Fund, Japan (to G.O.), The Ichiro Kanehara Foundation for the Promotion of Medical Sciences and Medical Care (to G.O), Yamaguchi Educational and Scholarship Foundation (to G.O).

ABBREVIATIONS

BDD, Boron-doped diamond.

REFERENCES

(1) Sigel, A.; Sigel, H.; Sigel, R. K. O. Interrelations between Essential Metal Ions and Human Diseases (Springer, Dordrecht, Netherlands, 2013).
(2) Gupta, J.; Qureshi, S. S. Potential Benefits of Methylcobalamin: A Review. *Austin J. Pharmacol. Ther.* **2015**, *3*, 1076.
(3) Wang, M.; Han, Y.; Fan, Z.; Zhang, D.; Wang, H. Therapeutic Effect on Idiopathic Sudden Sensorineural Hearing Loss with Duration of Onset More Than 3 Months. *Indian J. Otolaryngol. Head Neck Surg.* **2013**, *65*, 61–65.
(4) Dallos, P.; Fay, R. R. The cochlea (Springer-Verlag, New York, USA, 1996).
(5) Elgoyhen, A. B.; Wedemeyer, C.; Di Guilmi, M. N. Efferent Innervation to the Cochlea (2019).
(6) Partearroyo, T.; Vallecillo, N.; Pajares, M. A.; Varela-Moreiras, G.; Varela-Nieto, I. Cochlear Homocysteine Metabolism at the Crossroad of Nutrition and Sensorineural Hearing Loss. *Front. Mol. Neurosci.* **2017**, *10*, 107.
(7) Bari, N. M.; Khan, Z. G.; Patil, D. D. Analytical Methodologies for Determination of Methylcobalamin: An Overview. *Austin J. Anal. Pharm. Chem.* **2016**, *3*, id1062.
(8) Szterk, A.; Roszko, M.; Małek, K.; Czerwonka, M.; Waszkiewicz-Robak, B. Application of the SPE reversed phase HPLC/MS technique to determine vitamin B12 bio-active forms in beef. *Meat Sci.* **2012**, *91*, 408–413.
(9) Kumudha, A.; Kumar, S. S.; Thakur, M. S.; Ravishankar, G. A.; Sarada, R. Purification, identification, and characterization of methylcobalamin from Spirulina platensis. *J. Agric. Food Chem.* **2010**, *58*, 9925–9930.
(10) Clark, J. J.; Sandberg, S. G.; Wanat, M. J.; Gan, J. O.; Horne, E. A.; Hart, A. S.; Akers, C. A.; Parker, J. G.; Willuhn, I.; Martinez, V.; Evans, S. B.; Stella, N.; Phillips, P. E. M. Chronic microsensors for longitudinal, subsecond dopamine detection in behaving animals. *Nat. Methods.* **2010**, *7*, 126–129.
(11) Wang, J. Electrochemical Glucose Biosensors. *Chem. Rev.* **2010**, *108*, 814–825.
(12) Birke, R. L.; Gu, R. A.; Yau, J. M.; Kim, M. H. Polarographic Catalytic Hydrogen Waves in Aquocobalamin and Methylcobalamin Solutions. *Anal. Chem.* **1984**, *56*, 1716–1722.
(13) Rubinson, K. A.; Itabashi, E.; Mark, H. B. Electrochemical Oxidation and Reduction of Methylcobalamin and Coenzyme B12. *Inorg. Chem.* **1982**, *21*, 3571–3573.
(14) Huang, Q.; Gosser, D. K. Electrochemical study of methylcobalamin determination of the reduction potential for a quasireversible system with a fast following reaction. *Talanta* **1992**, *39*, 1155–1161.
(15) Lexa, D.; Saveant, J. M. The Electrochemistry of Vitamin B12. *Acc. Chem. Res.* **1983**, *16*, 235–243.
(16) Suzuki, A.; Ivandini, T. A.; Yoshimi, K.; Fujishima, A.; Oyama, G.; Nakazato, T.; Hattori, N.; Kitazawa, S.; Einaga, Y. Fabrication, characterization, and application of boron-doped diamond microelectrodes for in vivo dopamine detection. *Anal. Chem.* **2007**, *79*, 8608–8615.
(17) Yang, N.; Yu, S.; MacPherson, J. V.; Einaga, Y.; Zhao, H.; Zhao, G.; Swain, G. M.; Jiang, X. Conductive diamond: Synthesis, properties, and electrochemical applications. *Chem. Soc. Rev.* **2019**, *48*, 157–204.
(18) Einaga, Y. Development of Electrochemical Applications of Boron-Doped Diamond Electrodes. *Bull. Chem. Soc. Jpn.* **2018**, *91*, 1752–1762.
(19) Panizza, M.; Cerisola, G. Application of diamond electrodes to electrochemical processes. *Electrochim. Acta.* **2005**, *51*, 191–199.
(20) Macpherson, J. V. A practical guide to using boron doped diamond in electrochemical research. *Phys. Chem. Chem. Phys.* **2015**, *17*, 2935–2949.
(21) Swain, G. M.; Anderson, A. B.; Angus, J. C. Applications of Diamond Thin Films in Electrochemistry. *MRS Bull.* **1998**, *23*, 56–59.
(22) Einaga, Y. Diamond electrodes for electrochemical analysis. *J. Appl. Electrochem.* **2010**, *40*, 1807–1816.

(23) Fierro, S.; Yoshikawa, M.; Nagano, O.; Yoshimi, K.; Saya, H.; Einaga, Y. In vivo assessment of cancerous tumors using boron doped diamond microelectrode. *Sci. Rep.* **2012**, *2*, 901.
(24) Cvačka, J.; Quaiserová, V.; Park, J. W.; Show, Y.; Muck, A.; Swain, G. M. Boron-Doped Diamond Microelectrodes for Use in Capillary Electrophoresis with Electrochemical Detection. *Anal. Chem.* **2003**, *75*, 2678-2687.
(25) Muna, G. W.; Quaiserová-Mocko, V.; Swain, G. M. Chlorinated Phenol Analysis Using Off-Line Solid-Phase Extraction and Capillary Electrophoresis Coupled with Amperometric Detection and a Boron-Doped Diamond Microelectrode. *Anal. Chem.* **2005**, *77*, 6542-6548.
(26) Park, J.; Show, Y.; Quaiserova, V.; Galligan, J. J.; Fink, G. D., Swain, G. M. Diamond microelectrodes for use in biological environments. *J. Electroanal. Chem.* **2005**, *583*, 56–68.
(27) Park, J.; Galligan, J. J.; Fink, G. D.; Swain, G. M. In Vitro Continuous Amperometry with a Diamond Microelectrode Coupled with Video Microscopy for Simultaneously Monitoring Endogenous Norepinephrine and Its Effect on the Contractile Response of a Rat Mesenteric Artery. *Anal. Chem.* **2006**, *78*, 6756-6764.
(28) Patel, B. A.; Bian, X.; Quaiserová-Mocko, V.; Galligan, J. J.; Swain, G. M. In vitro continuous amperometric monitoring of 5-hydroxytryptamine release from enterochromaffin cells of the guinea pig ileum. *Analyst* **2007**, *132*, 41-47.
(29) Patel, B. A. Continuous amperometric detection of co-released serotonin and melatonin from the mucosa in the ileum. *Analyst* **2008**, *133*, 516-524.
(30) Ogata, G.; Ishii, Y.; Asai, K.; Sano, Y.; Nin, F.; Yoshida, T.; Higuchi, T.; Sawamura, S.; Ota, T.; Hori, K.; Maeda, K.; Komune, S.; Doi, K.; Takai, M.; Findlay, I.; Kusuhara, H.; Einaga, Y.; Hibino, H. A microsensing system for the in vivo real-time detection of local drug kinetics. *Nat. Biomed. Eng.* **2017**, *1*, 654–666.
(31) Lovander, M. D.; Lyon, J. D.; Parr, D. L.; Wang, J.; Parke, B.; Leddy, J. Review—Electrochemical Properties of 13 Vitamins: A Critical Review and Assessment. *J. Electrochem. Soc.* **2018**, *165*, G18–G49.
(32) Qiu, Q.; Dong, S. Rapid determination of kinetic parameters for the electrocatalytic reduction of dioxygen by vitamin B12 adsorbed on glassy carbon electrode. *Electrochim. Acta.* **1993**, *38*, 2297–2303.
(33) Zagal, J. H.; Aguirre, M. J.; Páez, M. A. O_2 reduction kinetics on a graphite electrode modified with adsorbed vitamin B12. *J. Electroanal. Chem.* **1997**, *437*, 45–52.
(34) Pourbaix, M. Atlas of Electrochemical Equilibria in Aqueous Solutions (National Association of Corrosion Engineers, 1974).
(35) Kasahara, S.; Natsui, K.; Watanabe, T.; Yokota, Y.; Kim, Y.; Iizuka, S.; Tateyama, Y.; Einaga, Y. Surface Hydrogenation of Boron-Doped Diamond Electrodes by Cathodic Reduction. *Anal. Chem.* **2017**, *89*, 11341–11347.
(36) Salazar-Banda, G. R.; Andrade, L. S.; Nascente, P. A. P.; Pizani, P. S.; Rocha-Filho, R. C.; Avaca, L. A. On the changing electrochemical behaviour of boron-doped diamond surfaces with time after cathodic pre-treatments. *Electrochim. Acta.* **2006**, *51*, 4612–4619.
(37) Yagi, I.; Notsu, H.; Kondo, T.; Tryk, D. A.; Fujishima, A. Electrochemical selectivity for redox systems at oxygen-terminated diamond electrodes. *J. Electroanal. Chem.* **1999**, *473*, 173-178.
(38) Kawamoto, K.; Oh, S. H.; Kanzaki, S.; Brown, N.; Raphael, Y. The Functional and Structural Outcome of Inner Ear Gene Transfer via the Vestibular and Cochlear Fluids in Mice. *Mol. Ther.* **2001**, *4*, 575–585.
(39) Lin, H.; Id, Y. R.; Lysaght, A. C.; Kao, S. Proteome of normal human perilymph and perilymph from people with disabling vertigo. *PLoS One* **2019**, *14*, e0218292.
(40) Yamane, K.; Usui, T.; Yamamoto, T.; Tsukamoto, T.; Soma, Y.; Yoshimura, N.; Nakano, S.; Manome, T.; Ishii, T.; Oda, N.; Ishii, M.; Umemura, S.; Ono, T. Clinical efficacy of intravenous plus oral mecobalamin in patients with peripheral neuropathy using vibration perception thresholds as an indicator of improvement. *Curr. Ther. Res.* **1995**, *56*, 656–670.
(41) Nitta, T.; Hata, M.; Gotoh, S.; Seo, Y.; Sasaki, H.; Hashimoto, N.; Furuse, M.; Tsukita, S. Size-selective loosening of the blood-brain barrier in claudin-5-deficient mice. *J. Cell Biol.* **2003**, *161*, 653–660.
(42) Nyberg, S.; Abbott, N. J.; Shi, X.; Steyger, P. S.; Dabdoub, A. Delivery of therapeutics to the inner ear: The challenge of the blood-labyrinth barrier. *Sci. Transl. Med.* **2019**, *11*, 1–11.
(43) National Center for Biotechnology Information. PubChem Database, (available at https://pubchem.ncbi.nlm.nih.gov/compound/24892769).
(44) Li, H.; Steyger, P. S. Systemic aminoglycosides are trafficked via endolymph into cochlear hair cells. *Sci. Rep.* **2011**, *1*, 159.

Table of Contents